

Calibrating M dwarf metallicities using molecular indices

Vincent M. Woolf^{1,2} and George Wallerstein¹

vwoolf@mail.unomaha.edu, wall@astro.washington.edu

ABSTRACT

We report progress in the calibration of a method to determine cool dwarf star metallicities using molecular band strength indices. The molecular band index to metallicity relation can be calibrated using chemical abundances calculated from atomic line equivalent width measurements in high resolution spectra. Building on previous work, we have measured Fe and Ti abundances in 32 additional M and K dwarf stars to extend the range of temperature and metallicity covered. A test of our analysis method using warm star – cool star binaries shows we can calculate reliable abundances for stars warmer than 3500 K. We have used abundance measurements for warmer binary or cluster companions to estimate abundances in 6 additional cool dwarfs. Adding stars measured in our previous work and others from the literature provides 76 stars with Fe abundance and CaH2 and TiO5 index measurements. The CaH2 molecular index is directly correlated with temperature. TiO5 depends on temperature and metallicity. Metallicity can be estimated to within ± 0.3 dex within the bounds of our calibration, which extends from roughly $[\text{Fe}/\text{H}] = +0.05$ to -1.0 with a limited extension to -1.5 .

Subject headings: stars: abundances — stars: late-type — stars: subdwarfs

1. Introduction

In Woolf & Wallerstein (2005) we reported the measurement of Fe and Ti abundances in 35 M and K dwarf stars using atomic line equivalent width measurements from high resolution, $\lambda/\Delta\lambda \approx 33\,000$, spectra. While the abundance survey provided useful results, it was clear that a method of estimating metallicity in cool dwarfs which works for fainter stars and which required less analysis effort was needed. Although low temperature dwarf stars are the most numerous stars in the Galaxy, their intrinsic faintness means that few of them are close enough for high resolution spectra to be measured. Because the abundances derived depend on the metallicity of the model atmosphere, several iterations are required for each star before the model and derived abundances match.

¹Astronomy Department, University of Washington, Box 351580, Seattle, WA 98195, USA

²Department of Physics, University of Nebraska at Omaha, 6001 Dodge St., Omaha, NE 68182, USA

Because low temperature main sequence stars, M dwarf and cooler, make up most of the baryonic mass of the Galaxy we must know their chemical compositions if we are to fully understand the chemical composition and evolution of the Galaxy. An open problem in modelling the chemical evolution of the Galactic disk is the ‘G dwarf problem’: fewer metal-poor G dwarfs are observed than models predict. The problem has been found to extend to stars with temperatures as cool as 4700 K (Flynn & Morell 1997). With a well-calibrated method to estimate M dwarf metallicities using low resolution spectra it will be possible to assemble a stastically significant sample of measurements and determine if the problem continues to stars with $T = 3500$ K or cooler.

Bonfils et al. (2005) combined abundances they measured in 20 binaries with M-dwarf secondaries and warmer primaries with the metallicity measurements from Woolf & Wallerstein (2005) to calibrate a M_K and $V - K$ vs metallicity relation. Because the relation depends on absolute magnitude it will be useful only for stars close enough for accurate parallaxes to be measured.

In this paper we report a metallicity calibration using the CaH2 and TiO5 indices. CaH2 and TiO5 are molecular indices which measure CaH and TiO band strengths in cool dwarf stars (Reid et al. 1995). These can be measured with lower resolution, $\lambda/\Delta\lambda \approx 3000$, flux calibrated spectra, and require only the measurement of relative flux levels in specified wavelength bands in spectra which have been corrected to zero velocity, which requires much less observational time and analysis effort than measuring and analyzing equivalent widths of atomic lines in higher resolution spectra. This method will allow metallicities to be estimated for stars at least 3 magnitudes fainter and considerably more distant than can be observed at high resolution. With 4-m class telescopes, stars fainter than $V = 16$ can be observed with reasonable exposure times at this resolution. For a $M_V = 10$ star this corresponds to a distance of about 160 pc, a greater distance than that for which reliable trigonometric parallaxes are available for large numbers of stars.

We have measured abundances in additional cool dwarfs to extend the range of temperature and metallicity which can be for which the metallicity relation can be calibrated. We have also used binaries with F, G, or K primaries and M dwarf secondaries to test our abundance analysis method and to extend the temperature and metallicity range.

2. Observations and reduction

We obtained spectra for the atomic line abundance analysis using the echelle spectrograph of the Apache Point Observatory (APO) 3.5-m telescope. The spectral resolution is $\lambda/\Delta\lambda \approx 33\,000$. The usable sections of the spectra cover a range from about 9800 Å to where the measured signal drops off in the blue, normally around 5000 Å for M dwarfs, and well below this for F and G dwarfs. Because the stars in our first paper included few low metallicity, $[Fe/H] < -0.5$, stars cooler than 3800 K, we obtained echelle spectra of additional M dwarfs with molecular band strengths which indicated they might have low metallicity.

To test the method we use to calculate abundances in M and K dwarfs, we observed a number

of stars in binaries where one member is an F, G, or early K dwarf and the other is a K or M dwarf with a temperature in the range covered our other stars. Most of these were selected from common proper motion pairs listed by Gould & Chanamé (2004). We also observed five Hyades M and K dwarfs.

We used the Dual Imaging Spectrograph (DIS) of the APO 3.5-m telescope to measure $\lambda/\Delta\lambda \approx 3000$ spectra of M and K dwarfs for which no TiO and CaH molecular band indices had been reported. The red arm of the spectrograph was set so the spectra cover the range $5950\text{\AA} < \lambda < 7650\text{\AA}$.

The echelle spectra were reduced using IRAF routines as described in Woolf & Wallerstein (2005). The DIS spectra were reduced using standard IRAF routines to subtract the bias, divide by flat-field spectra, reduce to one-dimensional spectra, apply HeNeAr lamp spectra wavelength calibration, and do standard star flux calibrations.

3. Analysis

M and K dwarf atmospheric parameters were estimated using V, K_s , and H photometric measurements (Cutri et al. 2003; Mermilliod et al. 1997) and parallax distances as described in Woolf & Wallerstein (2005). The magnitudes and parallaxes of the M and K dwarfs observed for this paper are listed in Table 1. For several stars we use the Hipparcos parallax of their brighter binary companion. Fe and Ti abundances were calculated for the M and K dwarfs using atomic line equivalent width measurements and NEXTGEN (Hauschildt et al. 1999) model atmospheres as described in Woolf & Wallerstein (2005).

We measured equivalent widths of Fe I, Fe II, Ti I, and Ti II lines in the F, G, and early K stars in binaries with an M or K dwarf using IRAF. Temperatures were estimated using Stromgren photometry (Alonso et al. 1996). Stellar masses and bolometric magnitudes were estimated using the theoretical M_V vs $B - V$ isochrones of Bertelli et al. (1994). We calculated stellar radii from the temperatures and bolometric magnitudes and calculated $\log g$ values from the radii and masses. We interpolated Kurucz model atmospheres (Kurucz 1993) to the derived T_{eff} and $\log g$ values. Microturbulent velocities for the F and G dwarfs were estimated using the empirical relation: $\xi = 1.25 + 8 \times 10^{-4}(T_{\text{eff}} - 6000) - 1.3(\log g - 4.5)\text{kms}^{-1}$ (Edvardsson et al. 1993). Fe and Ti abundances were calculated from the model atmospheres and the measured equivalent widths using the current version of the LTE stellar analysis program MOOG (Snedden 1973). The exception to this procedure was HIP 13642, where T_{eff} was estimated from the isochrones because no Stromgren photometric data were available.

The CaH2 and TiO5 molecular indices are ratios of the average flux levels in specified wavelength regions. We calculated the indices from the flux-calibrated DIS spectra using the wavelength regions defined by Reid et al. (1995).

4. Results

4.1. Chemical abundances

The atmospheric parameters and the Fe and Ti abundances derived for the 32 cool dwarf stars in Table 1 are listed in Table 2. The metallicity $[M/H]$ parameter listed is the effective metallicity after correcting for the effect of non-solar α -element to Fe abundance ratios as described in Woolf & Wallerstein (2005). The quoted abundance uncertainties include the effects of uncertainty in temperature, gravity, and microturbulence and the scatter of abundances determined from different lines in the same star. The temperature and gravity uncertainties listed in Table 2 are the uncertainties derived from uncertainties in the input parallax and photometry data and do not include the effects of possible systematic errors, which could possibly be as large as about ± 100 to 200 K for the temperature uncertainty and ± 0.3 to 0.4 for $\log g$.

To test our method of calculating abundances in cool dwarf stars we observed binaries with a cool dwarf secondary and a warmer dwarf primary. These were selected to have large enough angular separations that each component could be observed individually. Most primaries were F or G dwarfs. We also observed five cool dwarfs in the Hyades. The rationale for this test is that members of a binary or a cluster which formed from the same material should have the same chemical composition. Diffusion and nuclear enrichment processes which can change photospheric abundances should not have any measurable effect in these unevolved stars. The model atmospheres and methods used to find abundances in F and G dwarfs are well established. The good agreement between solar system meteoritic and solar photosphere abundances for most elements is evidence that the photospheric abundances calculated for solar-type stars using these models and methods are reasonable. If our method for calculating abundances in cool dwarfs is accurate then the abundances should agree with those calculated for their warmer binary or cluster companions.

The binary abundances are compared in Table 3 and Figure 1. The reported F and G dwarf abundance uncertainties include the effects of uncertainty in temperature, gravity, microturbulence, and the scatter of abundances determined from different lines. Temperature uncertainties due to uncertainties in the Stromgren photometry of the warm stars are less than 40 K. The temperature uncertainty and the uncertainties in determining the mass and bolometric magnitude for the warm stars correspond to $\Delta \log g < 0.10$. We find that the the binary and cluster Fe I abundances agree to within the combined uncertainties except for those with cool dwarfs with $T_{\text{eff}} < 3500$ K, which are indicated by open circles in the figure. The same pattern is seen for the Ti I abundances except that HD 18143B, BD+19 1185B, BD+17 791C, and LP 13-691 have abundance estimates a bit smaller than their warmer companions, even allowing for the uncertainties. Our method of measuring chemical abundances in cool dwarfs appears to provide accurate results for stars with temperatures greater than 3500 K. A weakness of this test is that we were unable to observe only one such binary with $[Fe/H] < -0.5$: low metallicity stars are less common, and identifying low metallicity cool dwarfs which are also in widely separated visual binaries with F or G dwarf companions is even more difficult.

The fact that we calculate similar abundances for both members of the binaries where the cooler member is warmer than 3500 K implies that the abundances we find for the warmer stars are not significantly affected by the possible problems caused by molecular bands. The metallicities of the binaries we studied were close to the solar metallicity. Stars of lower metallicity would be less affected by weak line blanketing.

There appears to be a systematic error causing the abundances calculated for stars cooler than 3500 K to be too large. It may be that the model atmospheres used do not sufficiently model the H₂O opacity which starts becoming much stronger at temperatures cooler than about 3500 K. It is also possible that increasing molecular band strengths at the cooler temperatures depress the apparent continuum in a molecular line haze, leading us to overestimate the atomic line equivalent widths. We note that because of this result, we are no longer certain of the abundances reported for LHS 450 in Woolf & Wallerstein (2005), the only $T_{\text{eff}} < 3500$ K star in that paper.

It should be possible, however, to calibrate our molecular index vs metallicity correlation to lower temperatures by including visual binaries. The last three binaries in Table 3 have secondaries which are too cool for abundances to be measured. We will assume that they have the abundances of their warmer companions.

4.2. Molecular index - metallicity calibration

The molecular indices and Fe abundances to be used for the metallicity calibration are listed in Table 4. The stars listed include all those from this paper and Woolf & Wallerstein (2005) for which molecular index data are available and 12 more from the other published reports. The abundances used for cool dwarfs in binaries with an F, G, or early K star are those of their warmer star. Abundances for stars in the Hyades or in a binary with two cool stars warmer than 3500 K are given by the average cluster or binary abundance. The uncertainties of the CaH2 and TiO5 index measurements are about ± 0.04 (Reid et al. 1995) or ± 5 to 10% (Zapetero Osorio & Martín 2004).

CaH2 is well correlated with effective temperature, as shown in Figure 2. TiO5 depends on temperature and metallicity. The locations of the stars in the CaH2 vs TiO5 plane and their [Fe/H] abundances are shown in Figure 3. Metallicity decreases to the lower right in the figure as expected: for a given temperature or CaH2 value, a smaller TiO5 value indicates a smaller metallicity.

We were unable to find an empirical polynomial fit to the data which corresponds well to the data. We have estimated the locations of equal-metallicity lines in CaH2 vs TiO5 by eye, as shown in Table 5 and Figure 4. Because the molecular band strengths decrease at higher temperatures, the fits start to converge for $\text{CaH2} \gtrsim 0.8$ or $T_{\text{eff}} \gtrsim 4000$ K. Molecular band strengths are poor indicators of metallicity at temperatures where the bands are very weak and the molecular index uncertainties correspond to large metallicity uncertainty. The ± 0.04 molecular index uncertainties correspond to an [Fe/H] uncertainty of about ± 0.3 through the entire region covered by our calibration grid.

5. Discussion

We have now determined the Fe and Ti abundances for 84 M and K dwarf stars using high resolution spectra and equivalent width abundance analysis. We have tested our analysis method using stars in binaries and a cluster and find that it appears to give reliable abundances for stars warmer than 3500 K.

When we include abundance data for 12 stars from other researchers we have 76 stars with measured Fe abundances and CaH2 and TiO5 indices. We have used these to create a rough molecular index – metallicity calibration.

The main shortcoming of our data is that we have few low metallicity stars with $T_{\text{eff}} < 4000$ K. Our data are not yet sufficient to determine whether the difficulty in identifying very low metallicity stars is partly caused by an ‘M dwarf problem’ similar to the G dwarf problem, where low metallicity stars are less common than predicted by Galactic star formation and chemical evolution models. At a given temperature, low metallicity stars are fainter than solar metallicity stars; they are “subdwarfs”. This means they must be physically closer to appear bright enough for a spectrum with sufficient signal to be obtained.

We have been granted time on the Hobby-Eberly Telescope to observe several M dwarf stars with CaH2 and TiO5 indices which indicate they have $[\text{Fe}/\text{H}] < -1.0$, but which are too faint to observe with APO. The abundances calculated from these spectra will help populate the low metallicity region of the CaH2 - TiO5 plane.

When the calibration is adequately defined it will be possible to estimate the metallicities of thousands of cool dwarf stars. Thousands of spectra of red dwarf stars have already been observed in the Sloan Digital Sky Survey. While the abundances estimated through a molecular index calibration will necessarily have larger uncertainties than those calculated through the analysis of atomic line strengths in high resolution spectra, they will be sufficient to allow statistical study of the relative numbers of cool dwarfs of different metallicities and a determination whether the G dwarf problem continues to lower masses, i.e. whether low metallicity M dwarfs are more scarce than models predict.

We thank Nicole Silvestri for obtaining some of the DIS spectra used for our molecular index measurements, Peter Hauschildt for continuing help with NextGen model atmospheres and Suzanne Hawley for helpful discussions about low mass subdwarfs. We thank Iain Reid for providing low resolution spectra to recheck the molecular indices of a couple stars. This research has made use of the SIMBAD database, operated at CDS, Strasbourg, France. This research has made use of NASA’s Astrophysics Data System Bibliographic Services. The authors gratefully acknowledge the financial support of the Kennilworth Fund of the New York Community Trust.

REFERENCES

- Alonso, A., Arribas, S., Martínez-Roger, C. 1996, *A&A*, 313, 873
- Bertelli, G., Bressan, A., Chiosi, C., Fagotto, F., Nasi, E. 1994, *A&AS*, 106, 275
- Bonfils, X., Delfosse, X., Udry, S., Santos, N.C., Forveille, T., Ségransan, D. 2005, *A&A*, accepted, doi:10.1051/0004-6361:20053046
- Cutri, R.M., et al. 2003, *The 2MASS All-Sky Data Release Explanatory Supplement*
- Edvardsson, B., Andersen, J., Gustafsson, B., Lambert, D.L., Nissen, P.E., Tomkin, J. 1993, *A&A*, 275, 101
- ESA 1997, *The Hipparcos and Tycho Catalogues (ESA SP-1200)* (Noordwijk: ESA)
- Flynn, C., Morell, O. 1997, *MNRAS*, 286, 617
- Fulbright, J.P. 2000, *AJ*, 120, 1841
- Gizis, G.E. 1997, *AJ*, 113, 806
- Gizis, G.E., Reid, I.N. 1997, *PASP*, 109, 1233
- Gould, A., Chanamé, J. 2004, *ApJS*, 150, 455
- Harrington, R.S., Dahn, C. C. 1980, *AJ*, 85, 454
- Hauschildt, P.H., Allard, F., Baron, E., 1999, *ApJ*, 512, 377
- Hawley, S.L., Gizis, J.E., Reid, I.N. 1996, *AJ*, 112, 2799
- Kurucz, R.L. 1993, *ATLAS9 Stellar Atmosphere Programs and 2 km/s grid*, CD-ROM No 13
- Mermilliod, J. -C., Mermilliod, M., Hauck, B. 1997, *A&AS*, 124, 349
- Paulson, D.B., Sneden, C., Cochran, W.D. 2003, *AJ*, 125, 3185
- Reid, I.N., Hawley, S.L., Gizis, J.E. 1995, *AJ*, 110, 1838
- Sneden, C.A., 1973, Ph.D. thesis, Univ. of Texas
- van Altena, W.F., Lee, J.T., Hoffleit, E.D. 1995, *The General Catalogue of Trigonometric Stellar Parallaxes*, 4th edn. L. Davis Press, Schenectady, NY
- Woolf, V.M., Wallerstein, G. 2005, *MNRAS*, 356, 963
- Zapetero Osorio, M.R., Martín, E.L. 2004, *A&A*, 419, 167

Facilities: APO

Table 1: M and K dwarf magnitudes and parallaxes

Star	Alternate name	Spectral type ^b	V	\pm^a	K _s	\pm	H	\pm	π (mas)	\pm (mas)	π source ^c
HIP 1386	GJ 3023	M2	11.518	0.020	7.241	0.011	7.499	0.023	42.65	2.77	Hip
HIP 17743	LHS 1594	M1	11.046	0.015	7.110	0.018	7.382	0.057	57.59	2.56	Hip
HIP 26801	HD 233153	M0.5	9.79	0.03	5.759	0.016	5.963	0.016	81.17	0.53	Hip
HIP 37798	GJ 287	K5	10.193	0.020	6.768	0.021	6.992	0.043	40.58	2.18	Hip
HIP 59514	HD 238090	M0	9.79	0.03	6.059	0.017	6.245	0.017	65.29	1.47	Hip
HIP 67308	GJ 1177A	K4	8.94	0.04	5.557	0.017	5.725	0.021	61.07	2.93	Hip
HIP 86087	GJ 685	M0.5	9.97	0.01	6.066	0.018	6.271	0.017	70.95	1.09	Hip
HIP 89490	HD 348274	M0	10.840	0.019	6.964	0.017	7.172	0.022	43.10	2.18	Hip
HIP 98906	LHS 482	sdM1.5	11.97	0.04	8.113	0.015	8.364	0.015	63.23	6.44	Hip
HIP 105932	GJ 828.2	M0.5	11.097	0.013	7.166	0.022	7.458	0.053	61.57	2.61	Hip
HIP 117383	GJ 907	M1	12.060	0.033	7.933	0.021	8.142	0.037	60.56	3.24	Hip
HD 7895B	LHS 1229	K7	10.705	0.029	7.190	0.013	7.369	0.025	36.16	1.00	Hip
HD 11964B	GJ 81.1B	K7	11.211	0.013	7.597	0.027	7.763	0.021	29.43	0.91	Hip
HD 18143B	GJ 118.2B	K7	9.80	0.04	6.170	0.036	6.299	0.038	43.71	1.26	Hip
HD 263175B	GJ 3409B	M0.5	12.17	0.01	8.184	0.014	8.428	0.031	40.02	1.22	Hip
HD 285804	...	K5	11.098	0.022	7.758	0.021	7.994	0.063	21.5	5.0	Hya
BD-1 293B	...	K	10.52	0.04	7.390	0.021	7.540	0.029	27.04	0.86	Hip
BD+17 719C	11.30	0.02	7.977	0.018	8.160	0.017	21.5	5.0	Hya
BD+19 1185B	LHS 1812	M1	13.40	0.04	9.822	0.028	10.011	0.021	14.86	2.50	Hip
BD+23 2207B	GJ 387B	M1	11.40	0.04	7.593	0.026	7.794	0.047	44.01	0.75	Hip
BD+24 4B	G 130-47	...	11.480	0.035	8.087	0.027	8.268	0.024	22.07	2.31	Hip
GJ 107B	BD+48 746B	M1.5	9.87	0.04	5.865	0.021	6.080	0.038	89.03	0.79	Hip
GJ 129	LHS 169	esdK7	14.16	0.04	10.819	0.018	11.012	0.023	30.0	2.3	Yal
GJ 1177B	...	K5	9.12	0.04	5.642	0.027	5.799	0.024	61.07	2.93	Hip
GJ 3212	...	M0.5	11.630	0.015	7.681	0.020	7.911	0.034
GJ 3278	...	M0.5	12.546	0.029	8.561	0.016	8.787	0.019	21.5	5.0	Hya
GJ 3290	...	M1.5	13.055	0.014	8.826	0.024	9.067	0.028	21.5	5.0	Hya
GJ 3825	LHS 364	esdM1.5	14.551	0.027	10.860	0.017	11.015	0.016	35.	5.	Nav
GJ 9722	LHS 64	sdM1.5	13.30	0.04	9.390	0.016	9.583	0.029	41.8	2.7	Yal
LHS 491	G 210-19	sdM1.5	14.74	0.03	10.869	0.024	11.102	0.027	20.4	4.2	Yal
LP 13-691	...	M0	11.84	0.04	8.224	0.018	8.390	0.018	21.5	5.0	Hya
2MASS 2203769-2452313	HIP 108923B	...	12.64	0.04	8.865	0.020	9.062	0.020	19.61	1.57	Hip

^aIn the absence of a reported V uncertainty estimate we used 0.04

^btaken from Gizis (1997), SIMBAD, Lee (1984), and Luyten (1979)

^cHip: ESA (1997), Yal: van Altena, Lee, & Hoffleit (1995), Hya: Hyades distance, Nav: Harrington & Dahn (1980)

Table 2: M and K dwarf parameters and abundances

Star	T_{eff} K	$\log g^a$	ξ km s ⁻¹	[M/H]	[Fe/H]	[Ti/H] ^b
HIP 1386	3600 ± 60	4.67 ± 0.11	1.0	0.15	0.16 ± 0.10	0.13 ± 0.09
HIP 17743	3685 ± 35	4.84 ± 0.07	1.0	-0.25	-0.30 ± 0.07	-0.22 ± 0.07
HIP 26801	3725 ± 20	4.71 ± 0.03	1.0	0.15	0.16 ± 0.09	0.09 ± 0.10
HIP 37798	4135 ± 45	4.67 ± 0.09	1.0	0.10	0.10 ± 0.09	0.11 ± 0.11
HIP 59514	3845 ± 25	4.69 ± 0.05	1.0	-0.03	-0.05 ± 0.08	-0.08 ± 0.09
HIP 67308	4085 ± 40	4.57 ± 0.08	1.4	-0.12	-0.16 ± 0.10	-0.26 ± 0.11
HIP 86087	3750 ± 15	4.71 ± 0.03	1.0	0.02	0.01 ± 0.08	0.01 ± 0.10
HIP 89490	3660 ± 20	4.56 ± 0.07	1.8	-0.44	-0.53 ± 0.08	-0.53 ± 0.10
HIP 98906	3670 ± 35	5.03 ± 0.18	1.0	-0.52	-0.62 ± 0.10	-0.22 ± 0.09
HIP 105932	3680 ± 40	4.87 ± 0.09	0.2	-0.30	-0.37 ± 0.05	-0.18 ± 0.04
HIP 117383	3560 ± 25	4.98 ± 0.09	1.0	-0.28	-0.33 ± 0.05	-0.38 ± 0.08
HD 7895B	4000 ± 30	4.69 ± 0.06	1.0	-0.04	-0.07 ± 0.08	-0.17 ± 0.10
HD 11964B	3930 ± 25	4.67 ± 0.06	1.0	0.00	-0.02 ± 0.09	0.02 ± 0.11
HD 18143B	3970 ± 45	4.52 ± 0.07	1.0	0.18	0.19 ± 0.11	0.07 ± 0.13
HD 263175B	3655 ± 20	4.89 ± 0.06	1.0	-0.20	-0.25 ± 0.07	-0.25 ± 0.08
HD 285804	4210 ± 60	4.57 ± 0.28	1.0	0.10	0.10 ± 0.09	0.07 ± 0.13
BD-1 293B	4310 ± 45	4.63 ± 0.07	1.75	-0.06	-0.09 ± 0.08	-0.20 ± 0.08
BD+17 719C	4185 ± 30	4.65 ± 0.27	1.0	0.05	0.04 ± 0.09	-0.05 ± 0.11
BD+19 1185B	3820 ± 40	4.77 ± 0.23	1.0	-0.78	-0.94 ± 0.07	-1.00 ± 0.08
BD+23 2207B	3740 ± 40	4.83 ± 0.05	1.0	-0.27	-0.33 ± 0.06	-0.28 ± 0.08
BD+24 4B	4085 ± 40	4.67 ± 0.04	1.0	-0.11	-0.15 ± 0.09	-0.11 ± 0.10
GJ 107B	3715 ± 20	4.77 ± 0.03	1.0	0.07	0.06 ± 0.08	0.06 ± 0.09
GJ 129	3965 ± 40	5.0 ± 0.5	1.0	-1.33	-1.66 ± 0.05	-1.34 ± 0.15
GJ 1177B	4015 ± 40	4.57 ± 0.09	1.2	-0.06	-0.09 ± 0.10	-0.20 ± 0.11
GJ 3212	3705 ± 25	5.0 ± 0.5	0.0	-0.06	-0.08 ± 0.05	0.01 ± 0.05
GJ 3278	3745 ± 20	4.69 ± 0.27	1.0	0.14	0.14 ± 0.10	0.12 ± 0.11
GJ 3290	3630 ± 15	4.75 ± 0.29	1.0	0.10	0.10 ± 0.11	0.02 ± 0.13
GJ 3825	3695 ± 25	5.0 ± 0.5	1.5	-1.09	-1.34 ± 0.10	-1.17 ± 0.13
GJ 9722	3595 ± 30	5.08 ± 0.12	1.0	-0.70	-0.83 ± 0.04	-0.75 ± 0.07
LHS 491	3630 ± 30	5.08 ± 0.32	1.0	-0.78	-0.93 ± 0.08	-0.68 ± 0.07
LP 13-691	3955 ± 35	4.65 ± 0.27	1.20	0.07	0.06 ± 0.11	-0.06 ± 0.13
2MASS 2203769- 2452313	3805 ± 35	4.72 ± 0.12	1.0	-0.09	-0.12 ± 0.09	-0.17 ± 0.10

^awe used $\log g = 5.0 \pm 0.5$ for the three stars where parallax was unavailable.

^bwe use $A(\text{Fe})_{\odot} = 7.45$, $A(\text{Ti})_{\odot} = 5.02$

Table 3. Binary and cluster abundances

Primary	T_{eff} K	$\log g$	ξ km s^{-1}	Fe I ^a	n lines	Fe II	n lines	Ti I	n lines	Ti II	n lines	Secondary	T K	Fe I	Ti I
HIP 9094	5140	3.86	1.39	7.39 ± 0.05	45	7.55 ± 0.11	16	4.86 ± 0.09	15	4.87 ± 0.13	3	HD 11964B	3930	7.43 ± 0.09	5.04 ± 0.11
HIP 12777	6200	4.25	1.60	7.43 ± 0.06	29	7.51 ± 0.09	7	4.98 ± 0.10	4	4.86 ± 0.10	2	GJ 107B	3710	7.51 ± 0.08	5.08 ± 0.09
HIP 13642	5150	4.52	0.50	7.80 ± 0.08	33	7.82 ± 0.10	17	5.54 ± 0.10	34	5.31 ± 0.13	2	HD 18143B	3970	7.64 ± 0.11	5.09 ± 0.13
HIP 13642	HD 18143C	3110	8.06	5.83
HIP 14286	5570	4.37	1.08	7.09 ± 0.07	29	7.10 ± 0.11	13	4.88 ± 0.09	16	4.80 ± 0.17	5	LHS 1494	3410	7.46	5.15
HIP 26779	5135	4.54	0.50	7.65 ± 0.06	26	7.81 ± 0.10	10	5.16 ± 0.09	16	5.41 ± 0.18	4	HIP 26801	3725	7.61 ± 0.09	5.11 ± 0.10
HIP 28671	5500	4.42	0.94	6.53 ± 0.08	34	6.38 ± 0.12	8	4.24 ± 0.12	5	4.11 ± 0.14	2	BD+19 1185B	3820	6.51 ± 0.07	4.02 ± 0.08
HIP 32423	4830	4.71	0.75	7.27 ± 0.06	29	7.40 ± 0.17	6	4.86 ± 0.09	17	4.98 ± 0.11	3	HD 263175B	3650	7.20 ± 0.07	4.77 ± 0.08
HIP 50384	6030	4.27	1.57	7.06 ± 0.05	24	7.08 ± 0.10	13	4.68 ± 0.09	6	4.68 ± 0.10	4	BD+23 2207B	3740	7.12 ± 0.06	4.74 ± 0.08
HIP 67308	4085	4.57	1.4	7.29 ± 0.10	15	4.76 ± 0.11	34	GJ 1177B	4015	7.36 ± 0.10	4.82 ± 0.11
HIP 86036	5710	4.38	1.17	7.34 ± 0.05	27	7.63 ± 0.10	8	4.99 ± 0.07	13	5.06 ± 0.13	4	HIP 86087	3750	7.46 ± 0.08	5.03 ± 0.10
HIP 114156	4250	4.69	1.0	7.38 ± 0.08	24	4.93 ± 0.10	39	G 275-2	3225	7.72	5.28
Hyades ^b	7.58 ± 0.01	5.18 ± 0.01	BD+17 719C	4185	7.49 ± 0.09	4.97 ± 0.11
Hyades	7.58 ± 0.01	5.18 ± 0.01	GJ 3290	3630	7.55 ± 0.11	5.04 ± 0.13
Hyades	7.58 ± 0.01	5.18 ± 0.01	GJ 3278	3745	7.59 ± 0.10	4.14 ± 0.11
Hyades	7.58 ± 0.01	5.18 ± 0.01	LP 13-691	3955	7.51 ± 0.11	4.96 ± 0.13
Hyades	7.58 ± 0.01	5.18 ± 0.01	HD 285804	4210	7.55 ± 0.09	5.09 ± 0.13
HIP 75069	5185	4.64	0.50	7.21 ± 0.04	27	7.30 ± 0.09	10	$4.79 \pm .07$	14	4.80 ± 0.14	4	LTT 14560
HIP 97675	6010	4.05	1.84	7.46 ± 0.06	28	7.40 ± 0.11	12	4.93 ± 0.09	5	4.88 ± 0.12	5	GJ 768.1B
HIP 99452	5250	4.55	0.58	7.48 ± 0.07	25	7.42 ± 0.07	8	5.32 ± 0.09	15	5.11 ± 0.17	4	GJ 283.2B

^aAbundances in this table are reported as $A(X) \equiv \log(N_X/N_H) + 12.00$ ^bHyades abundances from Paulson et al. (2003)

Table 4. Abundances and molecular indices for calibration

Star	T_{eff}	[Fe/H]	CaH2	TiO5	Fe source ^a	Index source ^b
HIP 1386	3600	0.16	0.56	0.59	1	1
HIP 17743	3685	-0.30	0.62	0.73	1	3
HIP 26801	3725	0.20	0.62	0.71	2	3
HIP 27928	4370	-0.73	0.97	0.96	3	1
HIP 37798	4135	0.10	0.80	0.89	1	3
HIP 59514	3845	-0.05	0.69	0.79	1	3
HIP 67308	4085	-0.13	0.73	0.93	2	1
HIP 86087	3750	-0.11	0.64	0.71	2	3
HIP 89490	3660	-0.53	0.66	0.77	1	3
HIP 98906	3670	-0.62	0.56	0.77	1	2
HIP 105932	3680	-0.37	0.67	0.73	1	3
HIP 117383	3560	-0.33	0.53	0.66	1	1
HD 7895B	4000	-0.07	0.76	0.85	1	3
HD 11964B	3930	-0.06	0.74	0.79	2	3
HD 18143B	3970	0.35	0.78	0.86	2	3
HD 18143C	...	0.35	0.41	0.40	2	3
HD 33793	3570	-0.99	0.59	0.81	3	2
HD 36395	3760	0.21	0.58	0.65	3	3
HD 88230	3970	-0.03	0.79	0.88	3	3
HD 95735	3510	-0.42	0.53	0.60	3	3
HD 97101B	3610	0.02	0.57	0.62	3	3
HD 119850	3650	-0.10	0.60	0.64	3	3
HD 178126	4530	-0.72	0.93	0.97	3	1
HD 199305	3720	-0.13	0.63	0.71	3	3
HD 217987	3680	-0.22	0.61	0.69	3	1
HD 263175B	3655	-0.18	0.60	0.72	2	3
HD 285804	4210	0.13	0.81	0.86	2	1
BD-1 293B	4310	-0.09	0.87	0.94	1	1
GJ 81.1B	...	0.09	0.74	0.79	4	3
GJ 105B	...	-0.19	0.41	0.38	4	3
GJ 107B	3715	-0.02	0.57	0.63	2	3
GJ 129	3965	-1.66	0.86	1.01	1	2
GJ 166C	...	-0.33	0.36	0.34	4	3
GJ 212	...	0.04	0.62	0.71	4	3
GJ 231.1B	...	-0.02	0.41	0.44	4	3
GJ 250B	...	-0.15	0.50	0.59	4	3
GJ 283.2B	...	0.03	0.40	0.39	2	3
GJ 297.2B	...	-0.09	0.49	0.56	4	3
GJ 324B	...	0.32	0.40	0.38	4	3
GJ 505B	...	-0.25	0.65	0.73	4	3
GJ 768.1B	...	0.01	0.44	0.45	2	3
GJ 783.2B	...	-0.16	0.40	0.39	4	3
GJ 797B	...	-0.07	0.48	0.53	4	3
GJ 1177B	4015	-0.13	0.70	0.91	2	1
GJ 3212	3705	-0.08	0.64	0.73	1	3
GJ 3278	3745	0.14	0.62	0.70	1	3

Table 4—Continued

Star	T_{eff}	[Fe/H]	CaH2	TiO5	Fe source ^a	Index source ^b
GJ 3290	3630	0.13	0.57	0.63	2	3
GJ 3825	3695	−1.34	0.60	0.98	1	2
GJ 9722	3595	−0.83	0.57	0.77	1	2
LHS 12	3830	−0.89	0.75	0.89	3	2
LHS 38	3600	−0.43	0.61	0.72	3	3
LHS 42	3860	−1.05	0.76	0.93	3	2
LHS 104	3970	−1.33	0.84	0.97	3	2
LHS 170	4230	−0.97	0.93	1.01	3	2
LHS 173	4000	−1.19	0.87	0.96	3	2
LHS 174	3790	−1.11	0.69	0.88	3	2
LHS 182	3870	−2.15	0.74	0.98	3	2
LHS 236	4040	−1.32	0.88	0.98	3	2
LHS 343	4110	−1.74	0.90	1.00	3	2
LHS 467	3930	−1.10	0.79	0.97	3	2
LHS 491	3630	−0.93	0.58	0.84	1	2
LHS 541	...	−1.54	0.44	0.71	5	3
LHS 1138	4620	−2.39	1.04	1.00	3	1
LHS 1482	4100	−1.88	1.00	0.94	3	1
LHS 1494	...	−0.36	0.46	0.48	2	3
LHS 1819	4670	−0.77	1.01	0.95	3	1
LHS 1841	4440	−1.47	1.04	0.97	3	1
LHS 2161	4500	−0.32	0.98	0.92	3	1
LHS 2715	4590	−1.16	0.97	0.99	3	1
LHS 3084	3780	−0.73	0.72	0.84	3	2
LHS 3356	3630	−0.20	0.61	0.69	3	3
LHS 5337	3780	−0.50	0.71	0.76	3	1
G 39-36	4400	−2.00	1.03	1.00	3	1
G 275-2	...	−0.07	0.41	0.41	2	3
2MASS 2203769-2452313	3805	−0.12	0.73	0.78	1	1
LTT 14560	...	−0.24	1.05	0.97	2	1

^a1: this paper, 2: this paper: binary or cluster abundance, 3: Woolf & Wallerstein (2005), 4: Bonfils et al. (2005), 5: Fulbright (2000)

^b1: this paper, 2: Gizis (1997), 3: Reid et al. (1995) and Hawley et al. (1996)

Table 5: CaH2, TiO5, [Fe/H] grid points

[Fe/H]=0.05		[Fe/H]=-0.50		[Fe/H]=-1.0		[Fe/H]=-1.5	
CaH2	TiO5	CaH2	TiO5	CaH2	TiO5	CaH2	TiO5
0.35	0.30	0.35	0.39
0.40	0.37	0.40	0.47
0.45	0.45	0.45	0.55	0.45	0.65
0.50	0.52	0.50	0.63	0.50	0.74
0.55	0.60	0.55	0.71	0.55	0.83
0.60	0.65	0.60	0.77	0.60	0.87
0.65	0.71	0.65	0.80	0.65	0.89
0.70	0.76	0.70	0.83	0.70	0.91	0.70	0.98
0.80	0.86	0.80	0.89	0.80	0.93	0.80	0.98

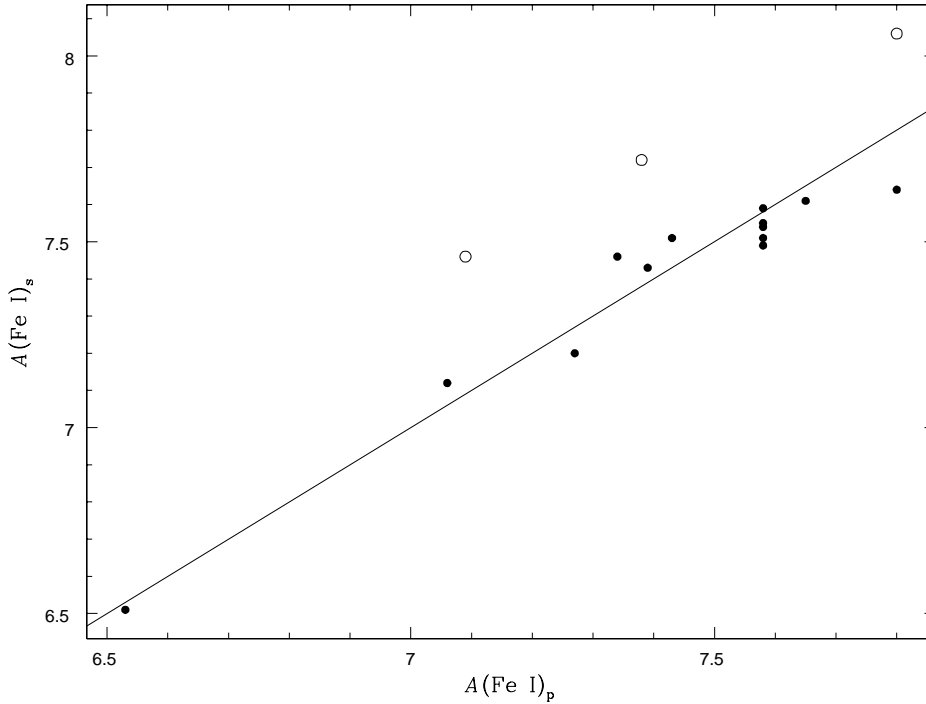


Fig. 1.— Cluster or binary warm star vs cool star Fe abundance comparison. Open circles indicate the secondary stars with $T_{\text{eff}} < 3500\text{K}$. The diagonal line indicates the location of perfect agreement.

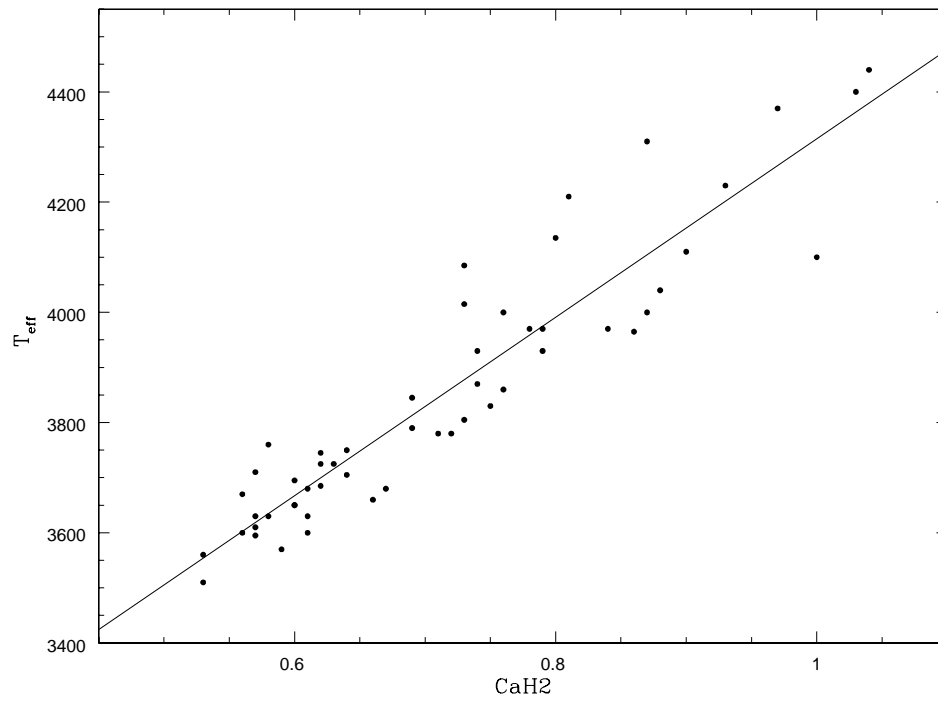


Fig. 2.— Temperature vs CaH2 index for program stars. The line is a least squares fit: $T_{\text{eff}} = (2696 + 1618 \times \text{CaH2}) \text{ K}$

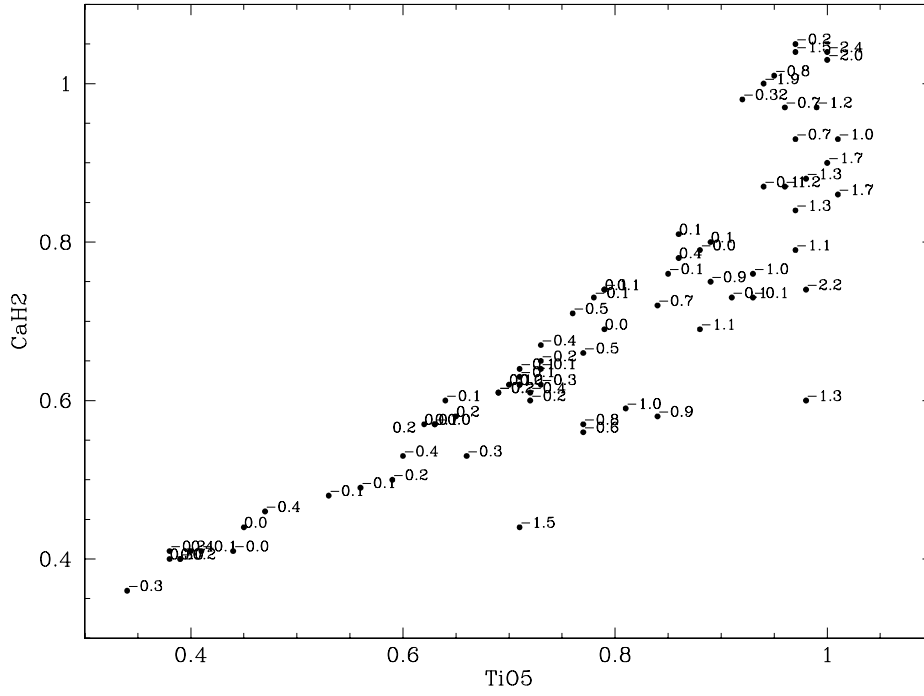


Fig. 3.— CaH2 vs TiO5. Numbers next to points indicate the $[Fe/H]$ values for each star.

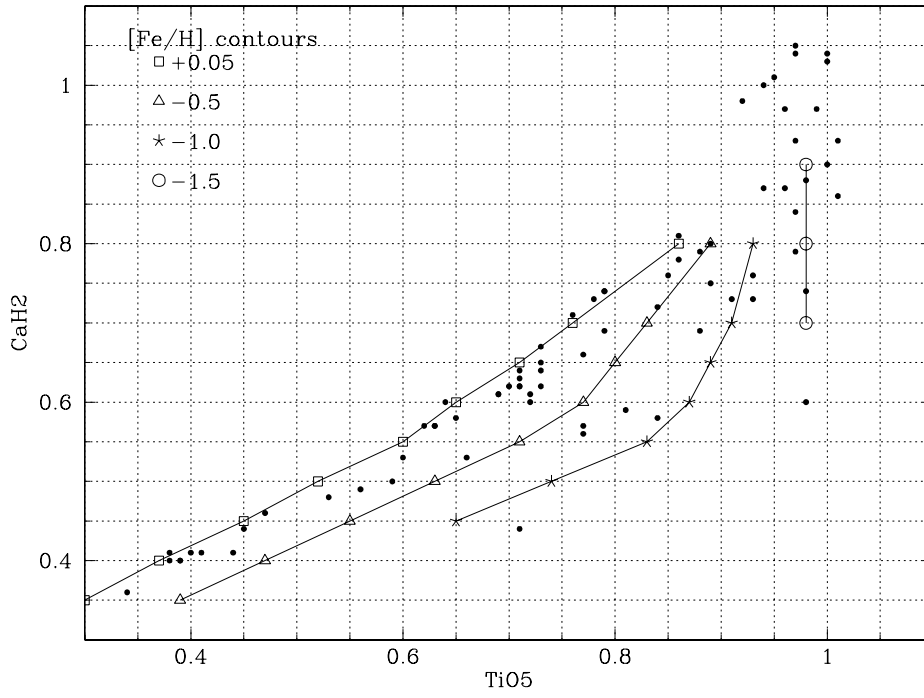


Fig. 4.— Equal-metallicity contours in CaH2 vs TiO5